TYPE II PRECURSOR AND X–RAY FLARE EMISSION

Andreas Klassen[1] and Silja Pohjolainen[2]

[1]Astrophysikalisches Institut Potsdam, Germany
[2]Tuorla Observatory, University of Turku, Finland

ABSTRACT

The formation of a radio emitting shock wave and its *precursor* above a flaring active region during the flare on 12 April 2001 is investigated. Using combined spectral and imaging observations of radio bursts with *Yohkoh* soft and hard X–ray imaging observations, we confirm earlier findings that the type II bursts are generated in association with and above the expanding soft X–ray loops. The type II *precursor* is identified as signature of a propagating disturbance which is later transformed into a type II burst. The observation of reverse drift bursts belonging to the *precursor* suggests that the *precursor* is an accelerator of electron beams and has a close relation to the soft and hard X–ray sources. We found that the speeds of the expanding loops, of the *precursor*, and of the type II exciter are comparable. The expanding loops however have the lowest speed.

Key words: Sun: flares; X–rays; shock waves.

1. INTRODUCTION

Type II bursts are radio signatures of propagating shock waves in the solar corona (Nelson & Melrose, 1985). They can be generated by two different mechanisms: the piston mechanism when coronal material propagate with a supermagnetosonic speed or the blast wave mechanism, i.e., a fast MHD shock generation due to sudden heating and pressure pulse during a flare (Vršnak, 2001). Observations suggest that the type II bursts in the middle corona result from flare processes (e.g. Wagner & MacQueen, 1983). The type IIs in the outer corona are rather associated with CMEs which act as a piston, driving a bow–shock wave (e.g. Gopalswamy et al., 1998).
Recent observations have shown that type II bursts are generated in association with rapidly expanding structures in the outskirts of flaring active regions (Klassen et al. 1999, Klein et al. 1999). The type II *precursor* signatures occur during the impulsive flare phase and are located between the flare release site and the type II position (Klassen et al. 1999). A *precursor* is defined as a sequence of fast–drift bursts which frequency envelope drift at a normalized drift rate, almost similar to the subsequent type II burst.

The dynamics of the type II *precursor* and its relation to the HXR sources are important but hitherto unknown. To investigate this problem we use combined observations of a strong type II burst on 12 April 2001 that had a very distinct type II *precursor*. The decimetric–decametric radio spectrum was observed by the Tremsdorf spectrograph (Mann et al. 1992). The radio imaging data was obtained with Nançay radioheliograph (NRH, Kerdraon & Delouis, 1997), the soft (SXR) and hard (HXR) X–ray observations from *Yohkoh* (Tsuneta et al. 1991; Kosugi et al. 1991). The very good time cadence of all the instruments give us the possibility to investigate the evolution of the type II *precursor*, the type II burst, and their relation to the impulsive flare, in particular to the HXR and SXR sources.

2. OBSERVATIONS

The radio event was associated with a X2.0 X–ray flare (start at 09:39, peak at 10:28 UT, SGD) in active region (AR) 9415, halo CME and proton event. The *type II burst precursor* (hereafter *precursor*) with subsequent type II burst is observed in the 700–200 MHz range at 10:14:20 – 10:16:35 UT (Fig. 1). Type II burst starts at 10:16:30 UT and shows multilane emission stripes in the 40–300 MHz range. In the early stage some of them overlap with each other, so that it is difficult to distinguish the exact relationship between the different lanes. But the main lanes show a distinct fundamental–harmonic relation.

The *precursor* shows the both fundamental and harmonic emission modes and starts around 450 MHz (fundamental mode). It consist of a group of fast reverse slope (hereafter RS) drift bursts with a restricted bandwidth. Their high and low frequency cut–off (envelope) drift to lower frequencies with a normalized drift rate similar to the following type II lanes. Fig. 1 (insert) displays an enlarged part of the *precursor* with a distinct sequence of RS bursts. After 10:16 UT the *precursor* is represented by dif-

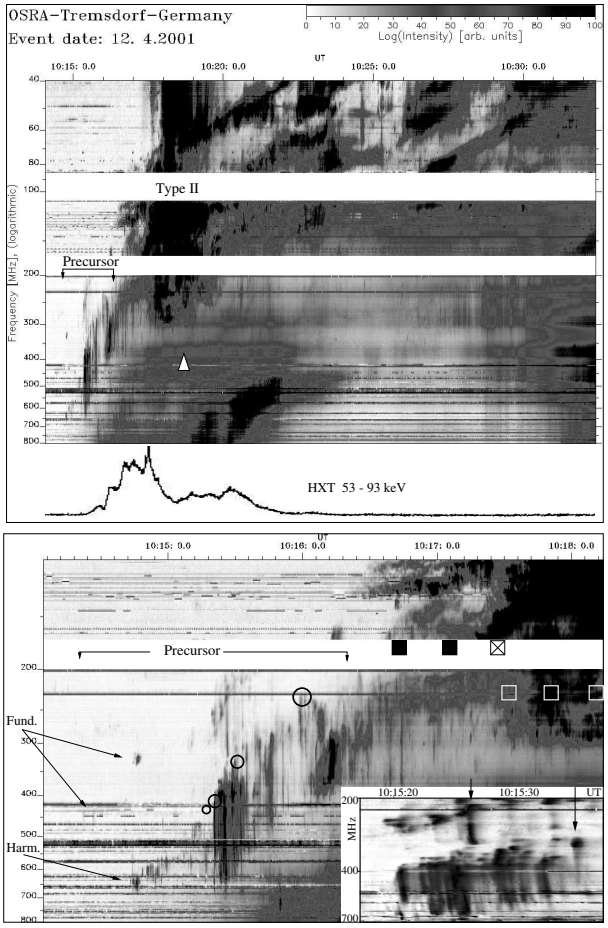

Figure 1. Dynamic radio spectrum of the event on 12 April 2001. **Top panel***: The event starts with a harmonic type II precursor, followed by a multilane type II burst. The precursor is accompanied by hard X–ray emission. At frequencies above those of type II a strong type IV occurs.* **Second panel***: hard X-ray light curve (HXT) in the range 53–93 keV.* **Bottom panel***: the precursor lanes consist mainly of a sequence of fast reverse slope (RS) drift bursts. Insert: Enlarged part shows the precursors (RS) bursts. Two of them are indicated by arrows.*

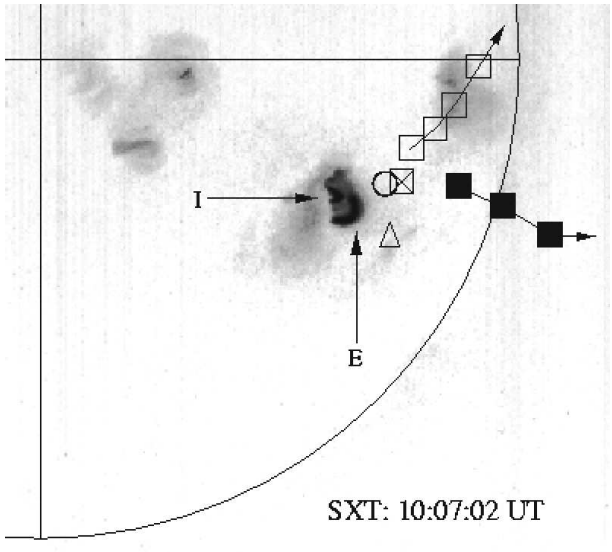

Figure 2. Pre–flare Yohkoh SXT image overlaid on radio source positions (centroids) at the time indicated by corresponding marks in Fig. 1. ◯ – precursors source position. The squares represent the positions and trajectories of different type II lanes. ■ – type II sources at 164 MHz 10:16:41–10:18:11 UT. □ – type II sources at 236 MHz at 10:17:31–10:19:11 UT. ⊠ – an additional type II source at 164 MHz at 10:17:21 UT. △ – type IV source at 432 & 327 MHz at 10:18:40 UT. Arrows point at the inner (I) and outer (E) loops. North is up, west is to the right.

ferent patches and fast drift bursts in both directions and it is partly overlapped by following type II lanes.

NRH observed at least three type II lanes at 236 & 164 MHz. Fig. 2 displays the source positions and the trajectories of different type II lanes overlaid on the pre–flare SXT image. Due to complex spectral structure and overlapping type II lanes, it is difficult to explain which spectral lanes belong to which observed sources. But generally the type II sources lie along two trajectories with respect to the flare site. The first trajectory shows a motion at a speed of $\geq$900–1400 km/s in the westward direction, belonging to the source of the first type II signature starting at 10:16:40 UT at 164 MHz. The second trajectory shows in the northwest direction and is traced by the source belonging to the lane which becomes visible later at about 10:17:30 UT at 236 MHz. This source occurs near and as extension of the *precursor* trajectory and has a speed of $\geq$1200–1400 km/s.

The *precursor* intersects all NRH observing frequencies except 164 MHz. Fig. 2 shows the centroids of the *precursor* sources, its low–frequency envelope, successively observed at 432, 327 and 236 MHz during the interval of 10:14:31–10:16:01 UT.
The *precursor* starts 60000 km above and slightly sidewards with respect to the inner SXR loops (I), and above the expanding outer SXR loops (E, Fig. 4). It moves northwestwards at a projected speed of 760–1090 km/s. The arrow connecting the open circles describes the outward motion of the *precursor* exciter, as traced by the brightening of the harmonic sources at successively lower frequencies.

During the period of 10:15:20–10:16:00 UT a few individual RS bursts of the *precursor* intersects two NRH frequencies, that allow us to determine the successive source positions and its direction of propagation (Fig. 1 insert, & 4). All measured trajectories of the RS bursts are aligned along the trajectory of the *precursor*. The individual RS bursts spread from the acceleration site to the SXR expanding outer loops and HXR loop–top sources. As an example the trajectories of two RS bursts observed at successive frequencies are presented in Fig. 4. The RS burst observed at 10:15:26 UT, showing J–shaped slope (Fig. 1 & 4), displays an unusual curved trajectory. At the beginning, it moves as other RS bursts towards the SXR loops. Later on, the source trajectory gets a sharp kink and shows a curved structure. Such a trajectory means that the electron beam was first injected into a loop–like structure and then it moved

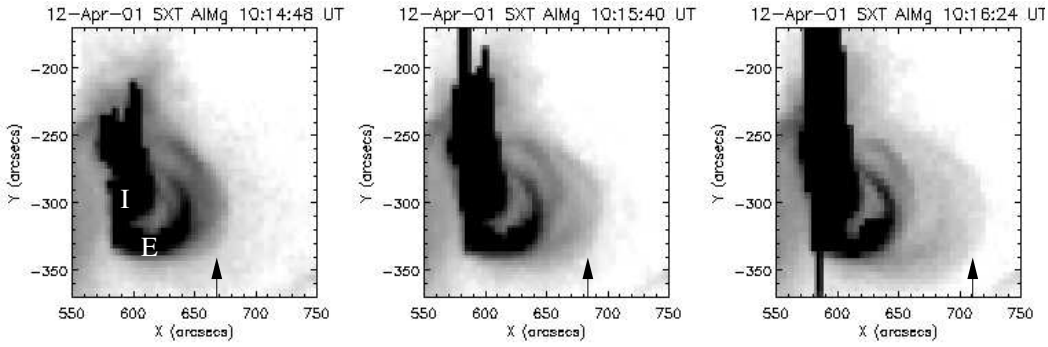

Figure 3. Time sequence of SXT images (AlMg filter) of AR 9415 during the type II precursor. The images show the outer loops (arrow–E) expanding in the north-west and west direction. The inner loops (I) become brighter and brighter without significant structural changes (they are partly saturated in the images).

along these loops. The speed of RS burst exciters can be derived from the drift rate in the spectrum using a model of density distribution along the burst trajectory. In our case this distribution is not known. Therefore we compare the drift rates of the *precursor* (D_f=4.0–5.3 MHz/s) and individual RS bursts (D_f=300–450 MHz/s) estimated at the same time and frequency range. Such a procedure is justified by the fact that they both occur in the same region and display the same trajectory. From the observed *precursor* speed of 760–1090 km/s we can estimate the speeds of individual RS bursts. Their speeds lie in the range of 55000–110000 km/s. That corresponds to 7–35 keV electron energies.

3. CORONAL STRUCTURES

3.1. Expanding SXR loops

In soft X–rays, before and during the flare the corresponding AR represents two compact systems of coronal loops: a) inner low–lying loops (hereafter inner loops, I) that are the brightest emitting structures, and b) outer high–lying loops (hereafter outer loops, E) located above of the inner loops (Fig. 2, 3). It seems that both systems had a common northern footpoint. The projected heights of both systems are about 28000 and 61000 km above the photosphere, respectively.

From the beginning at 10:14 UT until 10:20 UT the inner loops become brighter and brighter. The loops brightened first in the northern leg and then the brightest emitting region shifted to the top of the loops. During this time interval the inner loops show no significant morphological changes in their structure (Fig. 3). In contrast, the outer loops showed essential structural changes and brightened gradually. During 10:14:00–10:14:12 UT they started to brighten and thicken. Later, at 10:14:26–10:14:48 UT the loops show splitting and/or part of them lift off and move to the west direction. The rest of these loops stay at the same place. The difference images at 10:14:42–10:14:18 and at 10:16:44–10:16:24 UT (Fig. 4) show the westward expanding loops and the bright loop front that reaches the image frame, on the right. It seems that the expanding loop front shows distinct acceleration in the 10:14:18–10:16:44 UT time interval, from about 410 km/s to 700 km/s.

3.2. HXR sources during the *precursor*

The hard X–ray light curve (Fig. 1) shows periodic rise during the flare and accompanies the *precursor*. In L– and M1–bands (14–23, and 23–33 keV), the flux reaches its maximum at 10:20.5 UT, while in M2– and H–bands (33–53, and 53–93 keV) earlier at 10:17.5 UT. At energies > 23 keV there are two main peaks, the first is more associated with the *precursor* and the second one with type IV burst above 400 MHz.

In general, there is a source located at the apex of the inner loops (loop–top source) in addition to the usually observed double footpoint sources. In L– and M1–bands the emission shows a long structure which matches the corresponding soft X–ray inner loops (Fig. 4). This structure has several maxima, while the loop–top source is dominant. After 10:16 UT the footpoints are also visible. The images at higher energy channels (M2– and H1–bands) show a typical double footpoint structure, in which two sources are located near the ends of the inner loops. In the impulsive phase, during the *precursor*, one more source in addition to the dominant loop–top source is found in the L– and M–bands. It brightens several times for 1-2 seconds, almost simultaneously in both bands, and it is located near the apex of the outer loops, at position x=640, y=–280, (Fig. 4).

4. RESULTS

- The *precursor* starts simultaneously with HXR emission and the expansion of SXR outer loops. It occurs above the SXR loops and moves from the AR with a speed of 760-1090 km/s.
- Individual RS bursts of the *precursor* display a movement along and vice versa the *precursor* trajectory, i.e. back towards the expanding loops and loop–top HXR sources. The RS bursts reach the front of the expanding loops where they are stopped or dumped.
- The sources of different type II lanes show a movement in different directions with a speed of 900–1400 km/s.

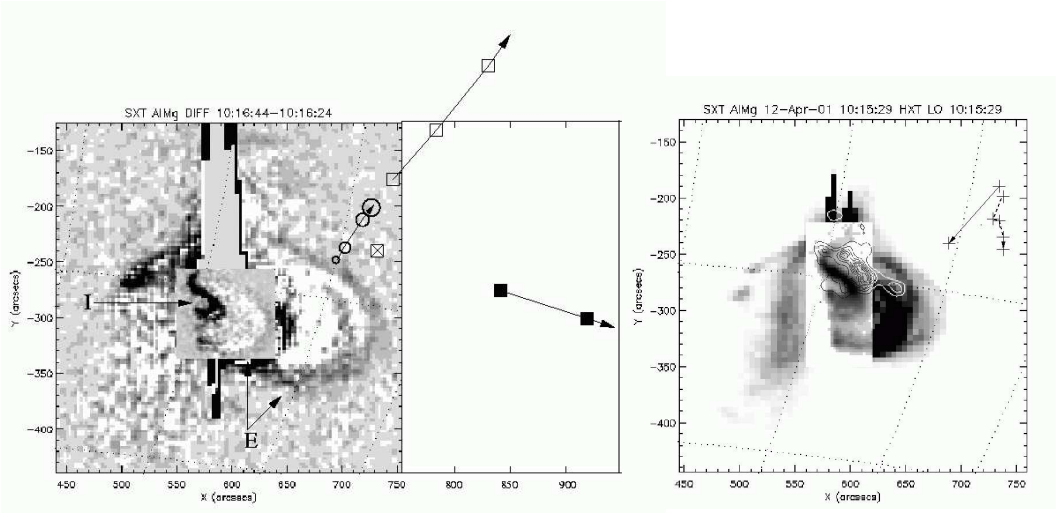

Figure 4. **Left**: *SXT difference image (AlMg filter, 10:16:44–10:16:24 UT) of the expanding outer loops superposed on the source positions of the precursor and the type II burst. Insert: SXT difference image (Be119 filter) at 10:14:41–10:14:18 UT. The circles show the source positions and the trajectory of the precursor at 432 (smaller circle), 410, 327 & 236 MHz (larger circle) at the times indicated by corresponding marks in Fig. 1. Boxes show the positions of different type II lanes (see Fig. 2).* **Right**: *The relation between SXR loops (gray scale), HXR sources (contours, 14–23 keV) and the precursor. HXR emission matches the corresponding inner loops while the loop–top source is dominant. During the impulsive flare phase and the precursor an additional HXR loop–top source appears near the apex of the outer loops (x=640, y=-280). The precursors RS bursts spread from the acceleration site to the SXR expanding outer loops and to the HXR loop–top sources. As an example the trajectories of two individual RS bursts are presented (indicated by arrows in insert of Fig. 1). Dashed arrow: RS burst at 236 & 327 MHz at 10:15:26 UT. Solid arrow: RS burst at 327 & 432 MHz at 10:15:35 UT.*

- The SXR images show two loop systems involved in the flare process. The inner loops (I) are stable, while the outer loops (E) show a rapid expansion with a speed of 400–700 km/s.
- HXR emission displays a triple source structure almoust coaligned with the inner loops. An additional source occurs during the *precursor* and the early impulsive flare phase. It is located near the apex of the outer loops at x=640, y=–280.

5. DISCUSSION

The spectral and spatial behaviour of the type II *precursor* and particularly its location between flaring loops, HXR sources and subsequent type II sources suggest that the *precursor* is a tracer of a propagating disturbance before it becomes the exciter of type II emission (Klassen et al. 1999). The timing of the *precursor* with respect to the start of loop expansion and to the onset of HXR emission shows that it appears at the very early impulsive flare phase. It means that the *precursor* appears almost simultaneously with the onset of HXR emission and the start of the loop expansion. Furthermore, the speed of the *precursor* exciter is larger than the speed of the expanding loops. Therefore, the *precursor* is not a consequence of the main energy release (HXR flare output) and possible not a consequence of the loops expansion. Only the initial destabilisation of the SXR loops (initial stress) can be involved as exciter of the *precursor*. Furthermore, the energy injection into the outer loops through the RS bursts of the *precursor* may play an important role by the destabilisation and initiation of the loop expansion, and by the occurence of the HXR loop–top sources. In each case the *precursor* represents an acceleration site of energetic particles.

ACKNOWLEDGMENTS

We are thankful to the Nançay Radioheliograph and *Yohkoh* SXT & HXT teams for data access.

REFERENCES

Gopalswamy, N., et al., 1998, JGR, 103, 307

Kerdraon, A., & Delouis, J.M. 1997, In: Trottet, G. (ed.) Lecture Notes in Physics 483, Coronal Physics from Radio and Space Observations, Springer, Berlin, p. 192

Klassen, A., et al. 1999, A&A 343, 287

Klein, K.-L., et al. 1999, A&A 346, L53

Kosugi, T., et al. 1991, Solar Phys., 136, 17

Mann, G., et al. 1992, ESA–Journal SP–348, 129

Nelson, G.J., & Melrose, D.B. 1985, in Solar Radiophysics, eds. McLean, D.J., & Labrum, N.R., (Cambridge Univ. Press, Cambridge), 333

Tsuneta, S., et al. 1991, Solar Phys., 136, 37

Vršnak, B. 2001, JGR, 106, 25291

Wagner, W.J., & MacQueen, R.M. 1983, A&A, 120, 136